FUEL EFFICIENT MODEL PREDICTIVE CONTROL OF PEM FUEL CELLS

Joshua Golbert and Daniel R. Lewin †

PSE Research Group, Wolfson Department of Chemical Engineering,
Technion I. I. T., Haifa 32000, Israel

Abstract: A dynamic PEM fuel cell model has been developed, taking into account spatial dependencies of voltage, current, material flows, and temperatures. The voltage, current, and therefore the efficiency, are dependent on the temperature and other manipulated variables, which can be optimized on the fly to improve fuel efficiency. Here we demonstrate that model predictive control can accurately satisfy setpoint changes in the power demand, while at the same time, reduce fuel consumption to maximize the efficiency.

Keywords: Fuel cells, model predictive control, fuel efficiency

1. INTRODUCTION

Fuel cells convert chemical potential into electrical power, and since they are not based on temperature differences, are not subjected to Carnot's limit of efficiency. Furthermore, as combustion is not involved, common pollutants such as sulphur dioxide and nitrous oxides are avoided. These advantages, together with the reduction of greenhouse gases and fuel consumption due to higher efficiencies and the possibility of alternative energy sources, have generated enormous interest in fuel cells for stationary as well as mobile applications.

Models of different complexity have been suggested, describing the performance of fuel cells under an array of conditions (Costamagna, 2001; Yi and Nguyen, 1998; Lee and Lalk, 1998). These models are then used to evaluate optimal schemes of external heating, water management and fuel composition.

The regulation of the transient response of fuel cells is important for vehicular applications, since the power demands fluctuate, and the fuel cell will not always be operating at the optimal steady state designed by its manufacturer. It is desirable to control the fuel cell so that acceptable response time for the power demand is ensured, while achieving high efficiencies. Dynamic models facilitate the design and testing of control systems. To this end, a dynamic empirical model for the transient response of a fuel cell was developed by Amphlett, et al. (1996). This is a lumped model with no spatial dependence. Kang et al. (2001) present an analysis of a dynamic model for a molten-carbonate fuel cell (MCFC) where the system is modelled as a collection of first order transfer functions with dead times. In previous work (Golbert and Lewin, 2004), a first-order, time dependent model of a fuel cell has been developed, which is fast enough to use for on-the-fly optimization of operating parameters to ensure convergence to required power. It has been demonstrated that model predictive control (MPC) relying on this model is more robust than standard linear control, especially in regions of high power density.

The objective of this paper is to demonstrate that MPC can be exploited to achieve both robust performance and improved fuel efficiency. We begin by briefly reviewing the reduced-order fuel cell model utilized by the controller. This is followed by a detailed description of the MPC formulation for fuel efficiency. Finally, we present the results obtained, comparing the performance with and without accounting for optimal efficiency.

2. FUEL CELL MODEL

The model developed by Golbert and Lewin (2004) is based on the concept presented by Yi and Nguyen (1998), in which a fuel cell is modelled along its channel, a schematic drawing of which is presented in Figure 1. The model accounts for heat transfer

† Author for correspondence. Email: dlewin@tx.technion.ac.il, URL: http://pse.technion.ac.il

between the solid and the two gas channels, and between the solid and cooling water. In addition, the water content is modelled, accounting for condensation and evaporation, water drag through the membrane, and water generation at the cathode. The model accounts for transients in the energy balance on the solid but all of the other equations are assumed to be at quasi-steady-state for each solid temperature profile. This spatially-dependent model is referred to as the "full-order" model, and is used to represent the true process in closed-loop simulations.

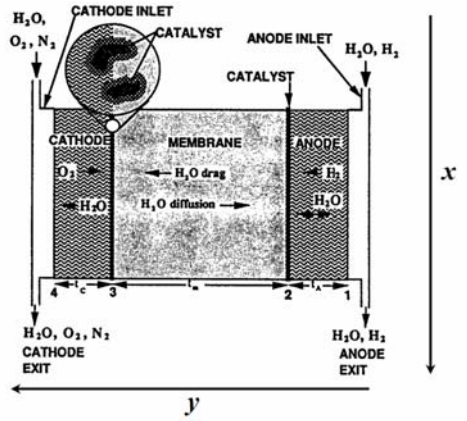

Fig. 1: Schematic diagram of fuel cell channel.

The main equations include the electrochemical Nernst equation accounting for overpotentials:

$$\frac{I(x)^2}{I_o^{\,2}}\exp\left(V_{act}\frac{2F}{RT}\right)-\frac{P_{H_2,s}(x)P_{O_2,s}(x)^{5/2}}{P_{H_2O,s}(x)}=0\,, \quad (1)$$

where:

$$V_{act}=\left(V_{cell}-V_{OC}^{o}+\frac{I(x)t_m}{\sigma_m(x)}\right)$$

$$P_{H_2,s}(x)=\left(P_{H_2,b}(x)-\frac{\delta I(x)}{2FD_{H_2}}\right)$$

$$P_{O_2,s}(x)=\left(P_{O_2,b}(x)-\frac{\delta I(x)}{4FD_{O_2}}\right)$$

$$P_{H_2O,s}(x)=\left(P_{H_2O,b}(x)+\frac{\delta I(x)}{2FD_{H_2O}}\right)$$

The solution of this equation gives the instantaneous current density. The concentrations of the reactant hydrogen and oxygen and the water product are governed by simple mass balances where their production/consumption rates are dependent on the current density:

$$\frac{dM_{H_2}(x)}{dx}=-\frac{h}{2F}I(x) \quad (2)$$

Finally, the water content is modelled by the rate of condensation in the respective channels:

$$\frac{dM_w^{l}(x)}{dx}=\frac{k_c h d}{RT(x)}\left\{\frac{M_w^{v}(x)}{\sum_i^{N_k}M_i(x)}P-P_w^{sat}(T)\right\} \quad (3)$$

and the rate of vapour accumulation; for instance, in the anode channel the vapour is consumed by water drag and well as by condensation:

$$\frac{dM_w^{v}(x)}{dx}=-\frac{dM_w^{l}(x)}{dx}-\frac{h\alpha(x)}{F}I(x) \quad (4)$$

The spatially-dependent model is simplified to enable rapid calculation for control and optimization purposes by lumping the spatial dependencies, which results in simple algebraic equations (for details, see Golbert and Lewin, 2004).

3. CONTROL OF A FUEL CELL

It is necessary to regulate the power output of the fuel cell to the levels required by the user. Since one of the applications for fuel cells will be automotive vehicles, we can expect the required load to change frequently in response to the drivers needs. In addition, there will be a degree of uncertainty in the behaviour of fuel cell components due to degradation of the materials, external temperatures and fuel composition and conditions. In spite of these uncertainties, the control system must be robust enough to satisfy the load demands by manipulating the input variables appropriately.

The input variables of such a system include the fuel and oxidant flowrates, composition and temperatures, coolant flowrate and temperature, anode and cathode pressures and, finally, the external resistance. The current density is often cited as an internal variable, using terms like "drawing current from the fuel cell" implying that it is determined arbitrarily by the operator. This, however, is akin to saying that liquid flowrate "is drawn" through a valve from an open tank. In reality, only the valve can be manipulated arbitrarily, which together with the liquid level determines the actual liquid flow. In practice, the valve is manipulated to satisfy a required flowrate. In the same fashion, the external resistance in a fuel cell is manipulated to satisfy a desired current density.

4. MPC FOR FUEL EFFICIENCY

Golbert and Lewin (2004) have shown that nonlinear MPC can satisfy changes in load demands robustly. The use of multiple variables can improve the response time of the system, with the target function to be minimized being the sum of square errors from the setpoint, with a penalty on the moves required in the manipulated variables. Clearly, there is potential for the optimizer to exploit the degrees of freedom inherent in the fuel cell design to improve the fuel-efficiency. In this regard, efficiency is defined as the ratio between the actual power produced and the heat of formation of the water produced if all the hydrogen feed is consumed:

$$\eta=\frac{hL\,P}{\Delta H\,M_{H_2}} \quad (5)$$

Since the MPC solves a minimization problem, a waste variable is defined, $1-\eta$, which is to be minimized by the optimizer. The most obvious way to improve the efficiency is to lower the feed flowrate. This is offset with the need for sufficient hydrogen concentration to achieve satisfactory volt-

age. An attempt by the controller to excessively reduce the hydrogen feed rate will result in an unbearably high concentration overpotential and thus compromise the power output. The objective function to be minimized is defined as the weighted sum of the performance (the difference between the set point and the actual power), the size of the control steps and the local efficiency over time:

$$J = \left(1 - w_{eff}\right) J_C + w_{eff}\left(1 - \eta\right) \tag{6}$$

where w_{eff} is a coefficient that expresses the desired trade-off between performance and efficiency, and J_C is the objective function for robust regulation:

$$J_C = \left(\underline{P(u)} - \underline{P_{set}}\right)^T \underline{\underline{W}} \left(\underline{P(u)} - \underline{P_{set}}\right) + \\ + \sum_i \underline{du_i}^T \underline{\underline{S_i}}\, \underline{du_i} \tag{7}$$

The optimization problem is subject to a number of constraints. First, each optimization variable has a maximum and minimum value. Since the actual variables for the optimization problem are defined in terms of changes from the previous value, the following definitions are required:

$$\begin{bmatrix} u_{1,k+1} \\ \vdots \\ u_{1,k+U} \\ \vdots \\ u_{n,k+1} \\ \vdots \\ u_{n,k+U} \end{bmatrix} \le \begin{bmatrix} u_{\max,1} \\ \vdots \\ u_{\max,1} \\ \vdots \\ u_{\max,n} \\ \vdots \\ u_{\max,n} \end{bmatrix} \tag{8}$$

However:

$$\begin{bmatrix} u_{1,k+1} \\ \vdots \\ u_{1,k+U} \\ \vdots \\ u_{n,k+1} \\ \vdots \\ u_{n,k+U} \end{bmatrix} = \begin{bmatrix} u_{1,k} \\ \vdots \\ u_{1,k} \\ \vdots \\ u_{n,k} \\ \vdots \\ u_{n,k} \end{bmatrix} + \overline{\underline{A_1}} \cdot \overline{du} \tag{9}$$

where

$$\overline{\underline{A_1}} = \begin{bmatrix} 1 & 0 & \cdots & & & & 0 \\ \vdots & \ddots & \ddots & & & & \vdots \\ 1 & \cdots & 1 & 0 & \cdots & & \vdots \\ 0 & \cdots & 0 & \ddots & \ddots & & \vdots \\ \vdots & \cdots & \cdots & 0 & 1 & 0 & 0 \\ \vdots & \cdots & \cdots & 0 & \vdots & 1 & \vdots \\ 0 & \vdots & \cdots & 0 & 1 & \cdots & 1 \end{bmatrix}, \quad \overline{du} = \begin{bmatrix} du_{1,k+1} \\ \vdots \\ du_{1,k+U} \\ \vdots \\ du_{n,k+1} \\ \vdots \\ du_{n,k+U} \end{bmatrix}$$

Hence,

$$\overline{\underline{A_1}}\, \overline{du} \le \begin{bmatrix} u_{\max,1} \\ \vdots \\ u_{\max,1} \\ \vdots \\ u_{\max,n} \\ \vdots \\ u_{\max,n} \end{bmatrix} - \begin{bmatrix} u_{1,k} \\ \vdots \\ u_{1,k} \\ \vdots \\ u_{n,k} \\ \vdots \\ u_{n,k} \end{bmatrix} = \overline{b_1} \tag{10}$$

In a similar fashion:

$$-\overline{\underline{A_1}} \cdot \overline{du} \le -\left(\begin{bmatrix} u_{\min,1} \\ \vdots \\ u_{\min,1} \\ \vdots \\ u_{\min,n} \\ \vdots \\ u_{\min,n} \end{bmatrix} - \begin{bmatrix} u_{1,k} \\ \vdots \\ u_{1,k} \\ \vdots \\ u_{n,k} \\ \vdots \\ u_{n,k} \end{bmatrix} \right) = \overline{b_2} \tag{11}$$

So far, the constraints ensure that the maximal values of the variables will not be exceeded at any step. If the fuel flowrate and the current density are to be manipulated there is a danger of the optimizer requesting an infeasible current density (above the limiting current density, which is largely influenced by concentration overpotential). Thus, for the sake of feasibility (as long as the current density is the input to the fuel cell model) a minimum ratio between the fuel and the current density must be enforced at all times:

$$M_{H_2} \ge ratio_{M_{H_2},I} \frac{hL}{2F} I = \phi I \tag{12}$$

where the ratio is a tuneable variable, which, in essence, ensures sufficient saturation of hydrogen. Translating from the values of u to the changes in u at each step and defining:

$$\overline{\underline{A_3}} \equiv \begin{bmatrix} -1 & 0 & 0 & 0 & \cdots & 0 & \phi & 0 & 0 \\ \vdots & \ddots & 0 & \vdots & \ddots & \vdots & \vdots & \ddots & 0 \\ -1 & \cdots & -1 & 0 & \cdots & 0 & \phi & \cdots & \phi \end{bmatrix}$$

and

$$\overline{b_3} \equiv \left(u_{M_{H_2},k} - ratio_{M_{H_2},I} \frac{hL}{2F} u_{I,k} \right) \begin{bmatrix} 1 \\ \vdots \\ 1 \end{bmatrix}$$

gives:

$$\overline{\underline{A_3}} \cdot \overline{du} \le \overline{b_3} \tag{13}$$

Note that when defining the matrix, the actual indices depend on the number of input variables being used.

Similar constraints must be defined for the oxygen/current ratio. However it is simpler to require that the oxygen always be in excess relative to the hydrogen flowrate by a certain ratio. Combining all of the constraints gives:

$$\begin{bmatrix} \overline{\underline{A_1}} \\ -\overline{\underline{A_1}} \\ \overline{\underline{A_3}} \end{bmatrix} \cdot \overline{du} \le \begin{bmatrix} \overline{b_1} \\ \overline{b_2} \\ \overline{b_3} \end{bmatrix} \tag{14}$$

This defines all of the constraints. For the sake of sensitivity, the variables are all scaled by their respective values entering the optimization:

$$du_i = du_i^* \cdot u_{i,nom} \tag{15}$$

or:

$$\overline{du} = diag\begin{pmatrix} u_{1,k} \\ \vdots \\ u_{1,k} \\ \vdots \\ u_{n,k} \\ \vdots \\ u_{n,k} \end{pmatrix} \cdot \overline{du^*} \qquad (16)$$

Substituting Eq. (16) into Eq. (14) gives:

$$\begin{bmatrix} \overline{\overline{A_1}} \\ -\overline{\overline{A_1}} \\ \overline{\overline{A_3}} \end{bmatrix} \cdot diag\left(\begin{bmatrix} u_{1,nom} \\ \vdots \\ u_{1,nom} \\ \vdots \\ u_{n,nom} \\ \vdots \\ u_{n,nom} \end{bmatrix} \right) \cdot \overline{du^*} \le \begin{bmatrix} \overline{b_1} \\ \overline{b_2} \\ \overline{b_3} \end{bmatrix} \qquad (17)$$

These are the linear constraints on the optimization variables. Furthermore, in cases where the hydrogen or oxygen flow rates are not optimized, the current is limited to the permitted ratio between the current and the constant value of the reactant flowrate. In this case, the upper limit on the current is either the set maximum current density (imposed by the user) or the value determined by the permitted current/reactant flow ratio, the lower of the two.

5. RESULTS

Applying MPC as defined above will lead to offsets from the desired power setpoint, since the objective function involves trade-offs between setpoint tracking error, usage of manipulated variables and the desire to maximize efficiency. However, in automotive applications, the offset from desired power delivery is not really important, since the fuel cell and its control system are not required to meet a specific power – rather the driver manipulates the power delivery as needed to meet the desired vehicle speed. Thus, it is appropriate to model the fuel-cell controller as a slave to a master controller (usually the driver), which supplies the power setpoint to the model predictive controller that then manipulates all the other variables (current density, flowrates, etc.). In such an arrangement, small offsets between the power setpoint and the actual power supplied by the fuel cell are acceptable. This type of setup is simulated using a PID controller and a simple model of a vehicle that obtains its power from the fuel cell. The model accounts for the vehicle acceleration based on the fuel cell power output, and the drag that is linearly dependent on the square of the velocity. Obviously, under normal circumstances the controller could be replaced by a human driver or cruise control. Figure 2 shows the Simulink® system diagram for this arrangement.

The following results compare the performance and efficiency of the PID/MPC system shown in Figure 2 when optimizing for performance exclusively and when optimizing for both performance and efficiency. The simulations start with the vehicle at a velocity of 30 km/hr, with a set point change to 90 km/hr imposed at t = 2 s.

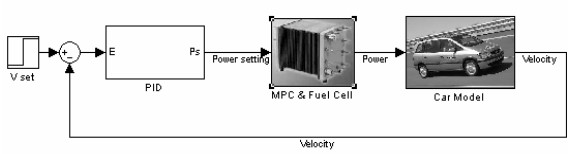

Fig. 2: Simulink® diagram for cascaded control system.

Figure 3 presents the results obtained when optimizing performance only, i.e., setting w_{eff} = 0. As can be seen, the velocity settles at 90 km/hr with no offset. The average fuel efficiency is 19%, with transient efficiency computed using Eq. (5). It is clear that although the initial conditions are at 46% efficiency, the changes in the power setpoint and changes in the input variables progressively reduce the efficiency to a value of only 14% by the end of the transient.

The results obtained for optimization accounting for efficiency as well as performance are presented in Figure 4. Note that a value of w_{eff} = 0.2 is used, with no improvements noticed for higher values. There are a number of points of interest. First, the average efficiency increases to 25.5%. This improvement is achieved is at the price of slightly more sluggish performance. The increased efficiency is obtained by the control that the MPC exerts on the hydrogen flowrate, reducing it when possible to conserve fuel.

Figure 5 shows the results obtained when optimizing for efficiency, again with a value of w_{eff} = 0.2, but now using the coolant temperature as an additional manipulated variable along with the current density and fuel flowrate. It is clearly seen that the extra degree of freedom afforded by the coolant temperature allows the controller to obtain almost the same performance as that in Figure 3 while increasing the average efficiency to 29%.

6. CONCLUSIONS

As has been previously established, model-based control scheme of a PEM fuel cell, relying on a reduced-order, nonlinear model of the process, can be used for robust regulation. In addition, as demonstrated in this contribution, since the controller adjusts a number of manipulated variables, it takes advantage of all of the degrees of freedom to simultaneously satisfy power demands while optimizing the fuel efficiency of the entire system. The results indicate that significant fuel savings can be achieved.

ACKNOWLEDGEMENTS

This research was supported by the Israel Science Foundation (Grant No. 25/03-15.4). The support of a Rieger Foundation Scholarship to Joshua Golbert for the academic years 2002-3 and 2004-5 are acknowledged with thanks.

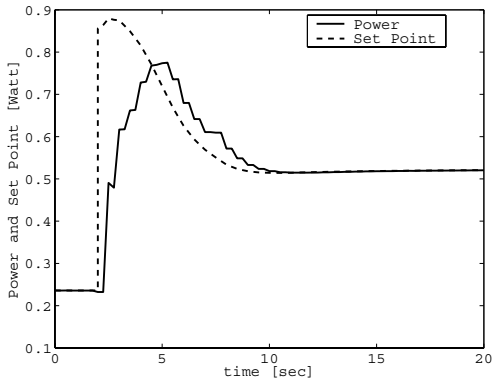

(a)

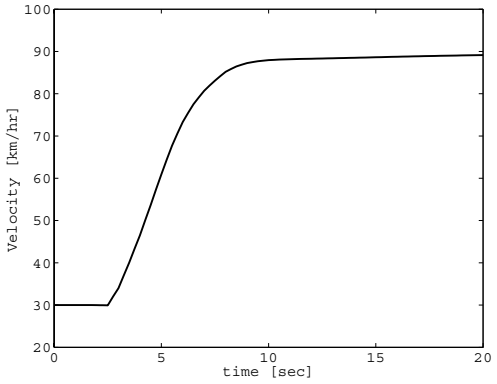

(b)

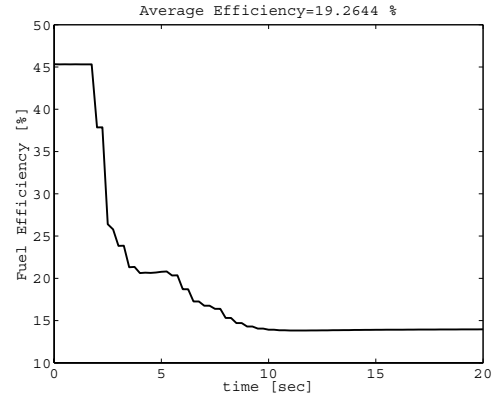

(c)

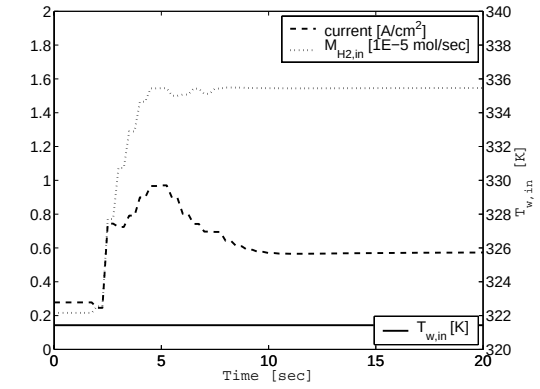

(d)

Fig. 3: Velocity control using cascaded PID/MPC optimizing for performance only: (a) power and setpoint, (b) vehicle velocity, (c) local efficiency from Eq. (5), (d) input current density, hydrogen flowrate and coolant temperature.

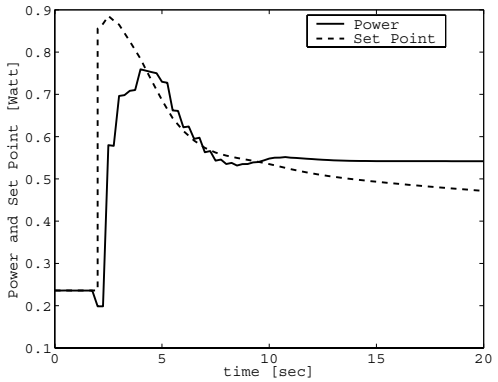

(a)

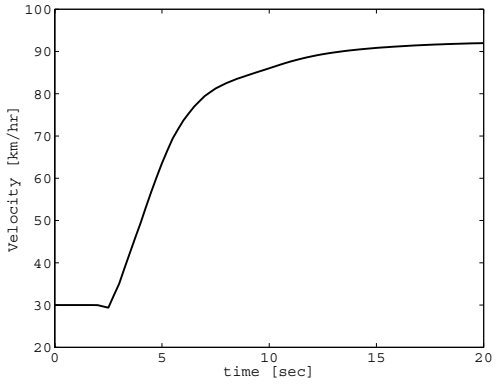

(b)

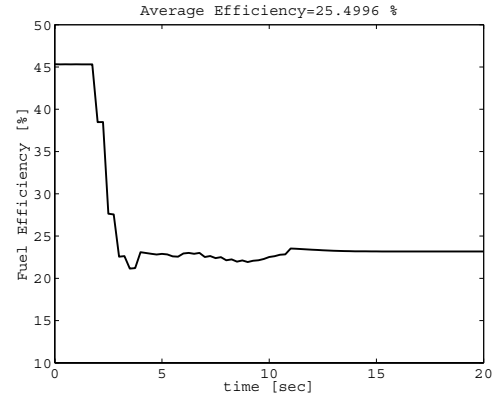

(c)

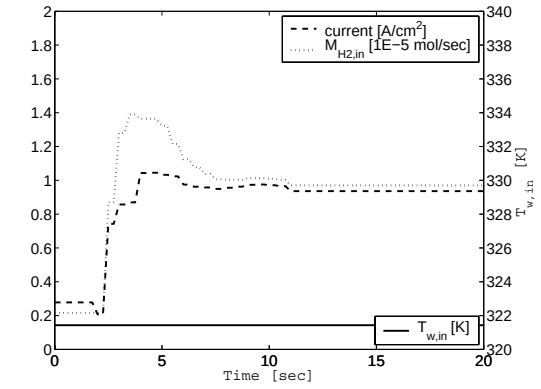

(d)

Fig. 4: Velocity control using cascaded PID/MPC optimizing for performance and efficiency, with captions as in Figure 3.

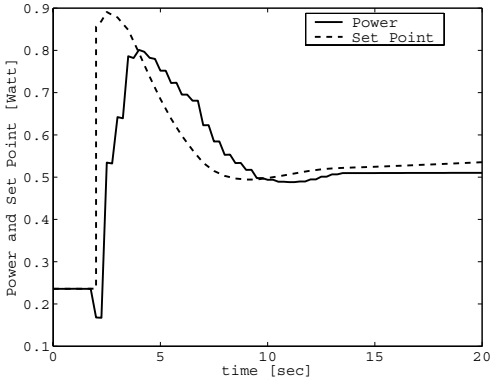

(a)

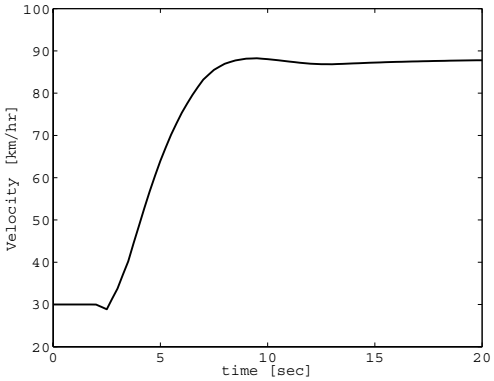

(b)

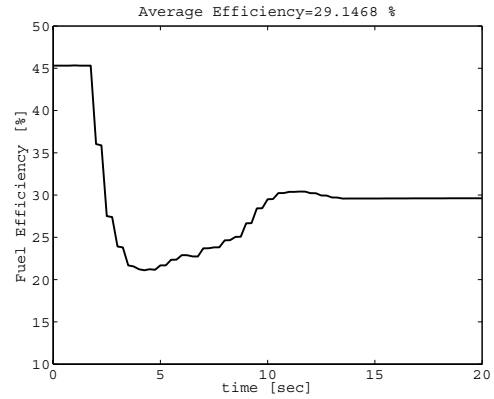

(c)

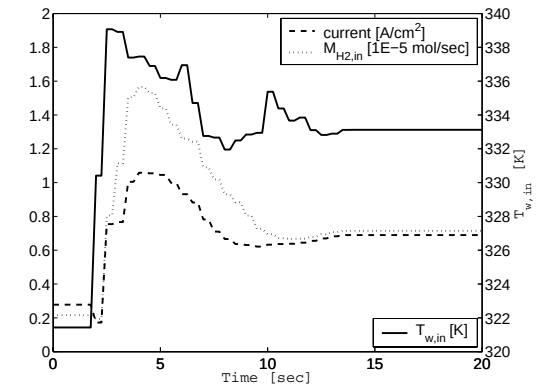

(d)

Fig. 5: Velocity control using cascaded PID/MPC optimizing for performance and efficiency, with captions as in Figure 3.

REFERENCES

Amphlett, J. C., R. F. Mann, B. A. Peppley, P. R. Roberge, and A. Rodrigues (1996). A Model Predicting transient Responses of Proton Exchange Membrane Fuel Cells, *J. Power Sources*, **61**, 183-188.

Costamagna, P. (2001). Transport Phenomena in Polymeric Membrane Fuel Cells, *Chem. Eng. Sci.* **56**, 323-332.

Kang, B., J. Koh, and H. Chun Lim (2001). Experimental study on the dynamic characteristics of kW-scale molten carbonate fuel cell systems, *J. Power Sources*, **94**, 51-62.

Golbert, J. and D. R. Lewin (2004). Model-based Control of Fuel Cells, *J. Power Sources*, **135**(1-2), 135-151.

Lee, J. H. and T. R. Lalk (1998). Modeling Fuel Cell Stack Systems, *J. Power Sources*, **73**, 229-241.

Yi, J. S. and T. van Nguyen (1998). An Along-the-Channel model for Proton Exchange Membrane Fuel Cells, *J. Electrochem. Soc.* **145**(4), 1149-1159.

NOMENCLATURE

a	Solid-gas heat transfer area per unit length along channel [cm]
b	Solid-coolant heat transfer area per unit length along channel [cm]
C_p	Solid heat capacity [J/gr K]
D	Diffusion coefficient [cm^2/sec]
e	Area of current per unit length along channel [cm]
f	Cross-section of solid in direction of reactant flow [cm^2]
F	Faraday constant [96,485 col/sec]
h	Channel width [cm]
I	Current density [amper/cm^2]
I_o	Exchange current density [amp/cm^2]
J	Objective function for MPC
L	Channel length [cm]
M	Molar flow [mol/sec]
P	Power density [Watt/cm^2]
P_i	Partial pressure of species *i* [atm]
R	Gas constant [8.314 J/mol K]
T	Temperature [Kelvin]
t_m	Membrane thickness [cm]
U	Heat transfer coefficient [W/cm^{2}K]
V	Voltage [volt]
V_{OC}	Open circuit voltage [Volt]
δ	Length of diffusion layer [cm]
η	Efficiency
ΔH	Enthalpy of overall reaction [J/mol]
ΔH_{vap}	Enthalpy of water condensation [J/mol]
ρ	Solid density [gr/cm^3]
σ	Membrane conductivity [(ohm cm)$^{-1}$]
S	Weight coefficient matrix for control moves
W	Weight coefficient matrix for setpoint tracking
w_{eff}	Weight coefficient of efficiency
u	Control variable value
du	Change in control variable value